Journal of Thermal Analysis, Vol. 47 (1996) 51-65

THERMAL CHARACTERIZATION BY PHOTODEFLECTION METHOD

M. Bertolotti, G. L. Liakhou, R. Li Voti and C. Sibilia*

Dipartimento di Energetica, Università di Roma 'La Sapienza', Via A. Scarpa 16, 00161 Roma, Italy and GNEQP of CNR, INFM, Italy and PF Materiali Speciali of CNR
*Technical University of Moldova, Stephan Cel Mare - 277012 Kishinev, Moldova

Abstract

The photodeflection technique is useful not only for thermal diffusivity measurements but also to supply a thermal imaging system. The experimental setup and the basic theoretical aspects for determining the temperature profile are discussed together with the experimental results on a semiconductor laser diode.

Keywords: photodeflection technique

Introduction

The photodeflection technique has been applied, since the beginning, to both the thermal and the optical characterization of solids [1]. The technique has been mainly developed in order to study the dynamic of the heat transfer in solids when thermal waves are induced by the time modulated pump laser absorption, which allows us to measure the thermal diffusivity according with the standard methodologies (crossing, phase and flash methods) [2–6]. Moreover photodeflection testing performed with different setups and various orientations of the sample has recently revealed large thermal anisotropy in polymer carbon fiber composites [7].

This technique is able also to determine the surface temperature profile in solids induced by any heat generation process (Joule, nonradiative deexcitation or recombination) giving informations on defects [8] and nonhomogeneities both buried and at the surface of the solid.

The good performances of this non destructive and contacless technique such as the high sensitivity to small temperature rises (10^{-3} K), at low room temperatures also (<200 K), the good spatial resolution (1–10 μm) and the opportunity to apply the technique to a wide set of samples with different geometries (rough samples) and to work in hostile environments make this method to be preferred rather than more common techniques, as for example, infrared thermography [9] or, more recently, the photothermal microscopy [10–12], this last based on the modulated laser induced photoreflectance.

0368–4466/96/ $ 5.00

John Wiley & Sons, Limited
Chichester

In the present work we review the main applications of the technique for thermal characterization of solids and introduce a new experimental setup which allows to get the temperature image, discussing the basic theoretical aspects to solve the inverse problem starting from the photodeflection data.

The experimental results are given for a semiconductor laser diode (double heterostructure AlGaAs/GaAs) periodically heated by the drive current [13–15]. The determination of the temperature profile at the surface, the thermal conductivity and diffusivity of the device are discussed.

Photodeflection

In general the photodeflection technique or 'mirage effect' concerns with the analysis of the deflection from its originary trajectory of a test laser beam (probe) travelling in a medium with a thermally induced refractive index gradient (Fig. 1). The thermal gradients are produced by a time modulated heating of the tested material in order to create thermal waves (usually produced by the absorption of pump laser beam or by current). The probe beam deflection produced in this way is given by the well-known formula [1, 3–8, 12–15]

$$\overline{\Phi} = \int_{\text{path}} \frac{\nabla_t n}{n} \, ds = \nabla_t \int_{\text{path}} \frac{1}{n}\left(\frac{dn}{dT}\right) T ds, \tag{1}$$

where n, (dn/dT), T, ∇_t denote the refractive index, the optothermal parameter, the temperature rise and the gradient transverse to the probe path respectively. The detection of the deflection angle is obtained by a position sensor (Fig. 1) connected with a lock-in amplifier and a PC, which also drives the mechanical stages providing the relative position between the laser beam and the tested sample to be varied.

In general two different methods can be distinguished depending on the time regimes of the heating (pulsed or harmonic regime) and a number of geometrical configurations depending on the probe beam path. In the collinear scheme (Fig. 1) the probe travels inside the sample (in situ) and perpendicular to the surface. On one hand large signals are obtained because the optothermal coefficient dn/dT of a solid sample is always larger than the one of the air. On the other hand this configuration can be applied only when the sample is transparent.

However, in the transverse configuration the probe laser beam is collimated by an optical system over the sample, so to skim in the air layer very close to the surface (Fig. 1). The deflection angle, in this scheme, has two components both of them normal to the beam path. The normal component to the solid surface (Φ_n) is usually larger but also more sensitive to the air thermal parameter, than the lateral one (Φ_l), so that it is not of good use for samples of low thermal diffusivity.

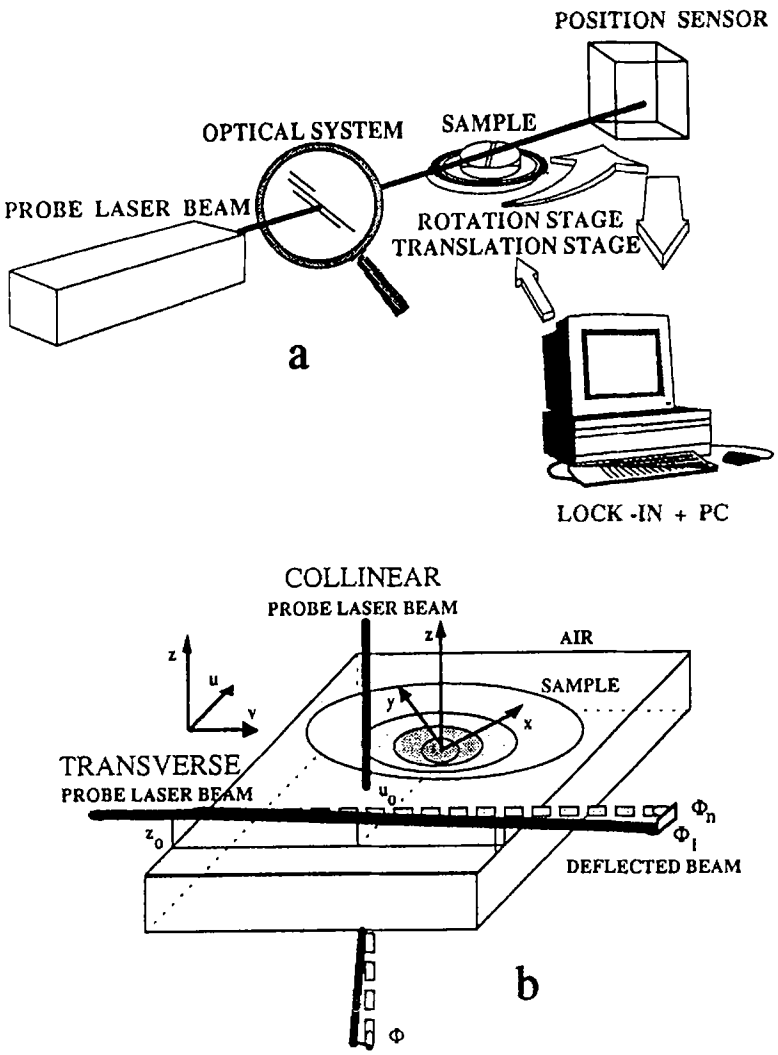

Fig. 1 Photodeflection configuration: (a) experimental setup; (b) photodeflection effect

Thermal diffusivity measurements

In general a very simple way to measure the thermal diffusivity of solids is by heating the sample with a laser pump beam focused in a small region and modulated in time with a chopper at a given frequency f (harmonic regime). In this case the typical behavior of the deflection angle of a probe laser beam travelling, in any configuration, at the minimum distance d from the heating point could be given by the relation [3, 4, 6]

$$\Phi = \Phi_o \, e^{-d/l} \cos(\omega t - d/l + \varphi) \tag{2}$$

where φ is a slowly varying function depending on geometrical coefficients and the spot sizes of the two lasers, which justifies the phase signal smoothing behavior for small values of d with respect to the spot-size, and l is a characteristic length that is connected to the thermal diffusivity of the sample through the relation

$$l = \sqrt{D/\pi f} + c, \tag{3}$$

where D is the thermal diffusivity, f the modulation frequency and c a constant which depends on geometrical coefficients only.

Therefore the calculation of the thermal diffusivity of the sample is possible directly from the deflection angle: in fact performing a scan in the d direction and looking at the phase of the deflection signal one usually finds a linear slope from which the characteristic length l is derived ('phase method'). In general further scans at different frequency are also needed. Also in this case a linear slope is found as a function of the inverse square root of the frequency. The thermal diffusivity could be obtained in this case by the formula [3–5]

$$D = \pi \left(\frac{\Delta l}{\Delta \sqrt{1/f}} \right)^2 \tag{4}$$

Photodeflection imaging

Photothermal deflection technique has been successfully applied also to supply an effective thermal imaging system in a wide range of applications.

The basic problem of any thermal imaging system based on photodeflection method, is that from the measurements (in any case or configuration), one gets the value of the average thermal gradient along the whole path of the probe laser beam (Eq. 1), but the local temperature values are not directly given. In order to reconstruct the surface temperature profile through the lateral component of the transverse signal, the inverse problem of Eq. (1) has to be solved.

In a traditional transverse photodeflection scheme (Figs 1, 2) a translation stage allows to perform a scan of the surface along the direction normal to the path ($u \equiv x$). In such way, sampling the scanned area with a spatial step Δ, a set of N measurements is given. Dividing the whole scanned area which we may assume to be a square without loss of generality, in a number $N \times N$ of squares whose temperature we wish to know, it is immediately clear that the solution of the inverse problem generally doesn't exist due to the inadequate number of data.

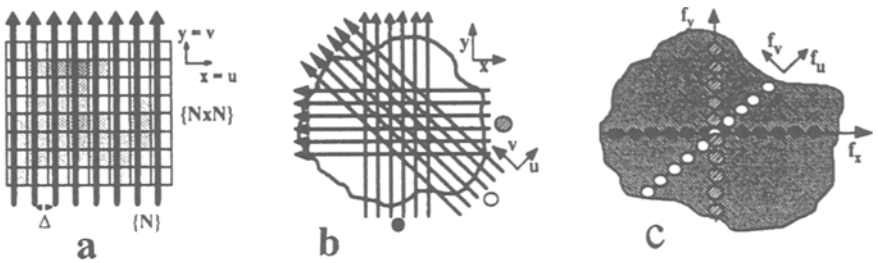

Fig. 2 Different types of scanning system: (a) traditional line scan; (b) non conventional scan; (c) Spatial Fourier transformed domain

An exception exists for the case that the surface temperature profile T_s has a radial symmetry (i.e. gaussian heating of a homogeneous and thermally isotropic sample) so that the general solution depending on two geometrical variables $T_s(x, y)$ degenerates in a single variable function $T_s(r)$.

In the general case the needed data for determining $T_s(x, y)$ could be provided by making a set of measurements $\{N\}$ for angles between the sample reference system (x, y, z) and the probe one (u, v, z). This new scanning system is obtained by means of two different stages to perform both translation and rotation of the sample surface.

In order to prove that in this way one is able to obtain a complete set of measurements to get the surface temperature profile $T_s(x, y)$, one needs to consider Eq. (1) for the case of lateral deflection angle, taking into account the spatial Fourier Transform of the surface temperature rise t_s and obtaining the relations

$$\Phi_t(u) = \left(\frac{1}{n}\,\mathrm{d}\frac{n}{\mathrm{d}T}\right)_{\text{air}} \int_{-\infty}^{\infty} \mathrm{d}v \frac{\partial}{\partial u} \int_{-\infty}^{\infty} \int_{-\infty}^{\infty} t_s(f_u, f_v) e^{2\pi j(f_u u + f_v v)}\, \mathrm{d}f_u \mathrm{d}f_v =$$

$$= \frac{\mathrm{d}n}{n\mathrm{d}T} \int_{-\infty}^{\infty} r 2\pi j f_u t_s(f_v = 0)\ e^{2\pi j(f_u u)} \mathrm{d}f_u \tag{5a}$$

$$t_s(f_v = 0) = -\frac{j}{2\pi}\left(\frac{\mathrm{d}n}{n\mathrm{d}T}\right)^{-1} F^{-1}[\Phi_t(u), f_u]/f_u \tag{5b}$$

where F^{-1} is the inverse Fourier Transform operator, f_u, f_v are the spatial frequencies along the directions u and v respectively. Note that Eq. (5a) and its inverse Eq. (5b) establish a simple relation between the deflection angle mea-sured by scanning the u axis and the transformed temperature along the transformed f_u axis (Fig. 2c). Finally rotating the xu angle in the range $(0, \pi)$, which also means the same rotation for the $f_x f_u$ angle, and repeating the scan along the u axis, t_s in all the domain (f_x, f_y) is given, from which $T_s(x, y)$ is eas-

ily calculated. In summary the consideration on the well posed inversion problem, justifies the choice of this useful scanning system.

Once the experimental setup has been defined, the next fundamental step is the research of a fast numerical algorithm to calculate directly from the sampled data the temperature profile at surface. Two different situations have to be discussed: a particular case in which a radial symmetrical temperature profile is expected, and the general case.

Profile with a radial symmetry

This is the typical case of the thermal response of an isotropical solid heated by a source with a radial symmetry. As previously indicated, the radial symmetry of $T_s(r)$ is kept also for $t_s(f)$ in the transformed domain. The main consequence is that, by rotating the angle xu, the same complete set of measurements is obtained. Therefore the great simplification, in the experimental setup, is to perform a scan along a whatever direction, as in traditional case, without repeating the procedure for different angles. In this case Eq. (5) could be rewritten as

$$T_s(r) = -\frac{1}{\pi}\left(\frac{dn}{ndT}\right)^{-1}\int_r^\infty \frac{\Phi_t(x)}{\sqrt{x^2 - r^2}}\,dx \leftrightarrow$$

$$\leftrightarrow \Phi_t(x) = 2\left(\frac{dn}{ndT}\right)\int_x^\infty \frac{dT_s(r)}{dr}\,\frac{x}{\sqrt{r^2 - x^2}}\,dr \qquad (6)$$

which represent the direct relationships between temperature and deflection and *vice versa*.

In a typical experiment, a scan along a line of finite dimension $L=N\Delta$ is performed, which provides a set of N data sampled at a given step Δ. If we calculate the temperature rise in the same spatial range with step Δ, by replacing in Eq. (6) the integral with the sum, the fast algorithm could be obtained

$$T_j = -\frac{1}{\pi}\left(\frac{dn}{ndT}\right)^{-1}\sum_{i=j}^{N}[\Phi_t]_i \ln\left(\frac{i+1+\sqrt{(i+1)^2 - j^2}}{i+\sqrt{i^2 - j^2}}\right) \quad j = 1\ldots N, \qquad (7)$$

where T_j is the calculated temperature rise at the position $r=j\Delta$ and $[\Phi_t]_i$ is the deflection angle at the position $x=i\Delta$. Note that any relation with the spatial step Δ or the dimension of the scanned line is completely absent. Therefore the evaluation of the error introduced in calculating the temperature with the algorithm in Eq. (7) becomes fundamental. The error is defined as

$$\varepsilon_j = |T_s(j\Delta) - T_j| \leq |T_s(N\Delta)| + \frac{1}{\pi}\left(\frac{dn}{ndT}\right)^{-1}\left[\Delta\left|\frac{d\Phi_t}{dx}\right|_{max} + |n|_{max}\right] \cdot$$

$$\cdot \ln\left(\frac{N + \sqrt{N^2 - j^2}}{j}\right), \tag{8}$$

where $T_s(j\Delta)$ is the correct value of the surface temperature rise, $|d\Phi_t/dx|_{max}$ is the maximum slope of the deflection angle as a function of the distance and $|n|_{max}$ represents the maximum noise value found in the scan. Note that in the evaluation of error, which depends on the position $j\Delta$, three different contributions can be distinguished:

1) the cut-off error $|T_s(N\Delta)|$ due to the (inevitable) truncation of the scanned line, whose value is directly given by the temperature at the last point of the scan. This error could be well controlled by stopping the scan where the deflection angle is negligible.

2) the sampling error (first term in the bracket) due to the deflection angle changes in the space between two successive measurements. This error is also improved by choosing the step Δ smaller than the scale of the deflection angle fluctuations.

3) the experimental error due to the sum of the noise of all the elements of the setup.

Therefore in order to decrease the total error, a simple way is given by decreasing the sampling step Δ. Note that Eq. (8) shows that this procedure is useful only when the sampling error is much larger than the experimental one, giving also an indication of the optimum Δ (when the two errors are comparable).

A different kind of error has also to be taken into account due to the fact that the probe laser beam travels in the air layer at a given height z from the surface. Therefore the probe is able to test mainly the temperature in a plane at a distance z from the sample surface and the found profile differs from the profile at surface. In that case we could introduce for the relative error the quantity

$$\varepsilon(z) = \frac{\int |T_z(r) - T(r)|\,dS}{\int |T(r)|\,dS}, \tag{9}$$

where the integrals are over the different planes. The evaluation of $\varepsilon(z)$ depends on the profile at surface, on the air thermal parameters and eventually on the frequency at which the sample is heated. The problem is here studied for two typical cases: a uniform heating and a point source heating. In Fig. 3 the rela-

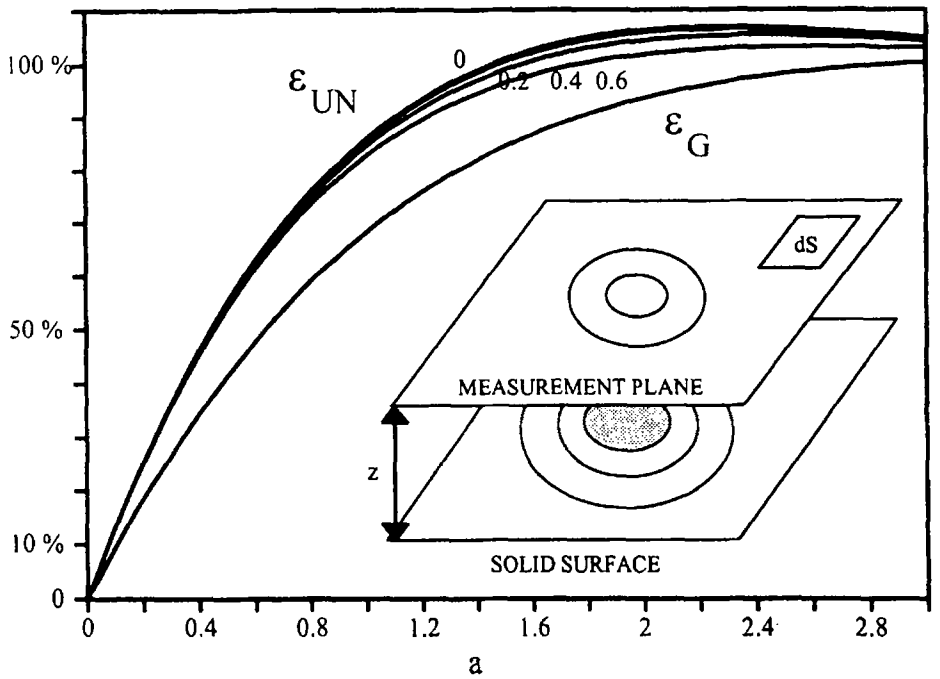

Fig. 3 Relative error *vs.* the ratio $a=z/l$ between the height z from the solid surface and the air thermal diffusion length for different heating sources: ε_G: Green point source heating; ε_{UN}: Uniform heating. The curves are relative to different values of the ratio between the probe beam size and z (0–0.2–0.4–0.6). In the insert the scheme of measurements

tive errors as a function of the normalized distance $a=z/l$, where l is the thermal diffusion length defined as $l = \sqrt{D_{air}/\pi f}$ being D_{air} the air thermal diffusivity, is shown for the case of uniform ε_{UN} and point source heating ε_G. In the uniform case the problem of the probe beam size has also been considered. All the curves that stands for different values of the ratio between the beam size and the distance z, differ very little from each other and also not too much from ε_G. As a conclusion, in order to decrease the relative error, the parameter z/l has to be kept as small as possible in any case, which means small values of z or low modulation frequencies.

Finally we test the algorithm in Eq. (8) for a simulation with a sample of given thermal parameters (thermal conductivity=0.01 W (cm K)$^{-1}$, thermal length=0.015 cm) heated by a time modulated gaussian pump beam (P= 10 mW, spot-size=0.01 cm, absorption=100 cm^{-1}). The dimension of the investigated zone is fixed to $r_{max}=0.128$ cm, while the number of sampling points N and consequently Δ has been considered a parameter. In the Fig. 4a the deflection and the correct and calculated temperature profiles are shown both in

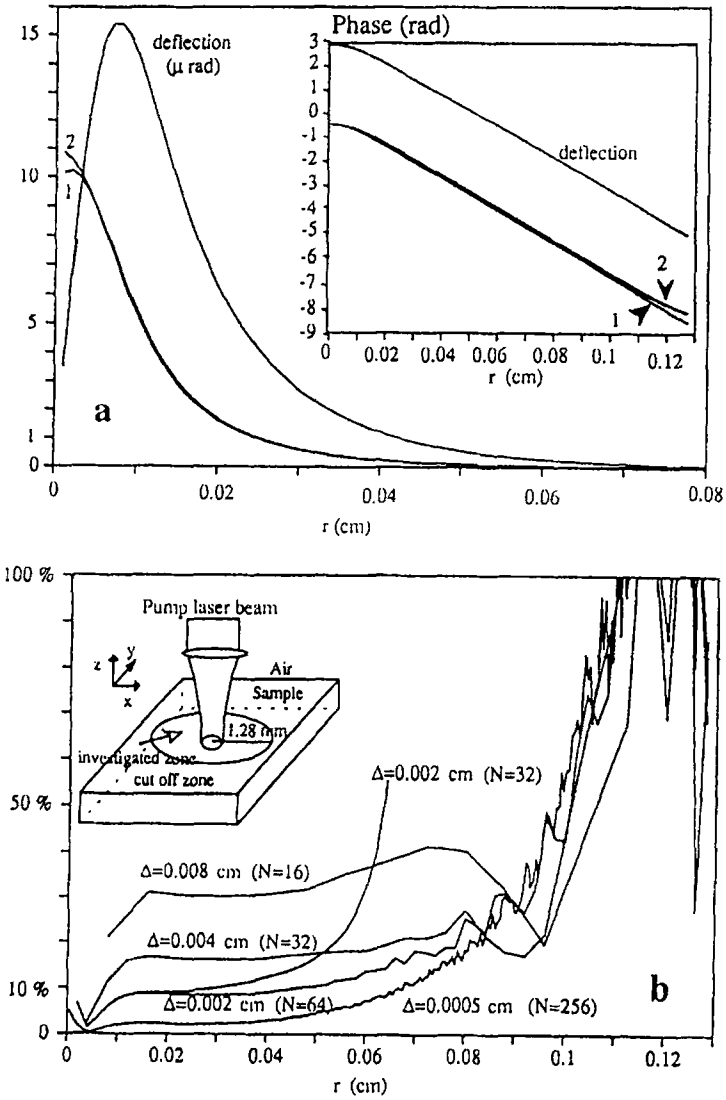

Fig. 4 (a) Temperature rise profiles and related deflection angle *vs.* the radial coordinate r: the curves of the amplitude of temperature are in Kelvin, the amplitude of deflection is in μrad. The curves of temperature are calculated directly from theory (1) and from Eqs (7), (2). Other used parameters are: $k=0.01$ W cm K^{-1}, absorption $a=100$ cm^{-1}, Pump beam power $P=10$ mW, spot-size $a=0.01$ cm, thermal length $l=0.015$ cm. In the box the phase in radian is reported for the temperature and deflection curves. (b) The relative error between temperature derived from theory and derived from Eq. (7) *vs.* the radial coordinate r: an experimental noise of one percent is added to the deflection data. The curves are relative to different number of points (16, 32, 64, 256) and different step Δ. In the insert the schematic representation of the setup

amplitude and in phase. The relative error between the temperature profiles in the case the set of N measurements is affected by an experimental noise of one percent, is also shown in Fig. 4b. Note in all curves the effect of truncation on the relative error. The figure confirms also the general idea that by increasing the number of samples N, the error decreases. The interesting result is that a relative error of 10% in the whole range where the temperature is not negligible (0–0.05 cm), is obtained for $N=64$ and a step $\Delta=20$ μm.

Profile without any spatial symmetry

Generally in case of deflection measurements performed with the scanning system described above, the inversion problem has a direct solution that links Φ to T_s by

$$T_s(r,\theta) = \frac{1}{2\pi^2}\left(\frac{dn}{ndT}\right)^{-1} \int_0^{\pi} d\varphi \int_{-\infty}^{\infty} \frac{\Phi_t(u,\varphi)}{r\cos(\theta-\varphi)-u}\, du, \tag{10}$$

where (r, θ) and (u, φ) are the polar coordinates in the sample (x, y) and in the probe beam (u, v) system respectively. Sampling the data both at a spatial Δ and angular $\Delta\varphi$ step the link between temperature $T_{ij}=T_s(i\Delta, j\Delta\varphi)$ and deflection $\Phi_{k,m}=\Phi(k\Delta, m\Delta\varphi)$ can be rewritten as

$$T_{ij} = \frac{\Delta_\varphi}{2\pi^2}\left(\frac{dn}{ndT}\right)^{-1} \sum_{k=-N/2}^{N/2} \sum_{m=0}^{M} \Phi_{k,m} \ln\left|\frac{k - i\cos[\Delta_\varphi(m-j+1/2)]}{k+1-i\cos[\Delta_\varphi(m-j+1/2)]}\right|$$

$$\begin{cases} k = -N/2 \ldots N/2 \\ i = 0 \ldots N/2 \end{cases} \begin{cases} m = 0 \ldots M/2 = \dfrac{\pi}{\Delta_\varphi} \\ j = 0 \ldots M \end{cases} \tag{11}$$

We have tested also this last algorithm for the same sample as above, heated by two gaussian pump beams (A, B), to provide the anisotropy of the temperature profile, placed as shown in Fig. 5a ($P(A)=20$ mW, $P(B)=10$ mW, size(A)= 0.005 cm, size(B)=0.01 cm). The results obtained for temperature profiles and relative error with a rotating angle step $\Delta\varphi$ of 15° and a spatial step $\Delta=10$ μm are excellent and prove the ability of this new sensitive method to get temperature profiles.

Experimental results

The experimental results of our investigation are reported for a laser diode double heterostructure AlGaAs/GaAs for a drive current of 70 mA harmoni-

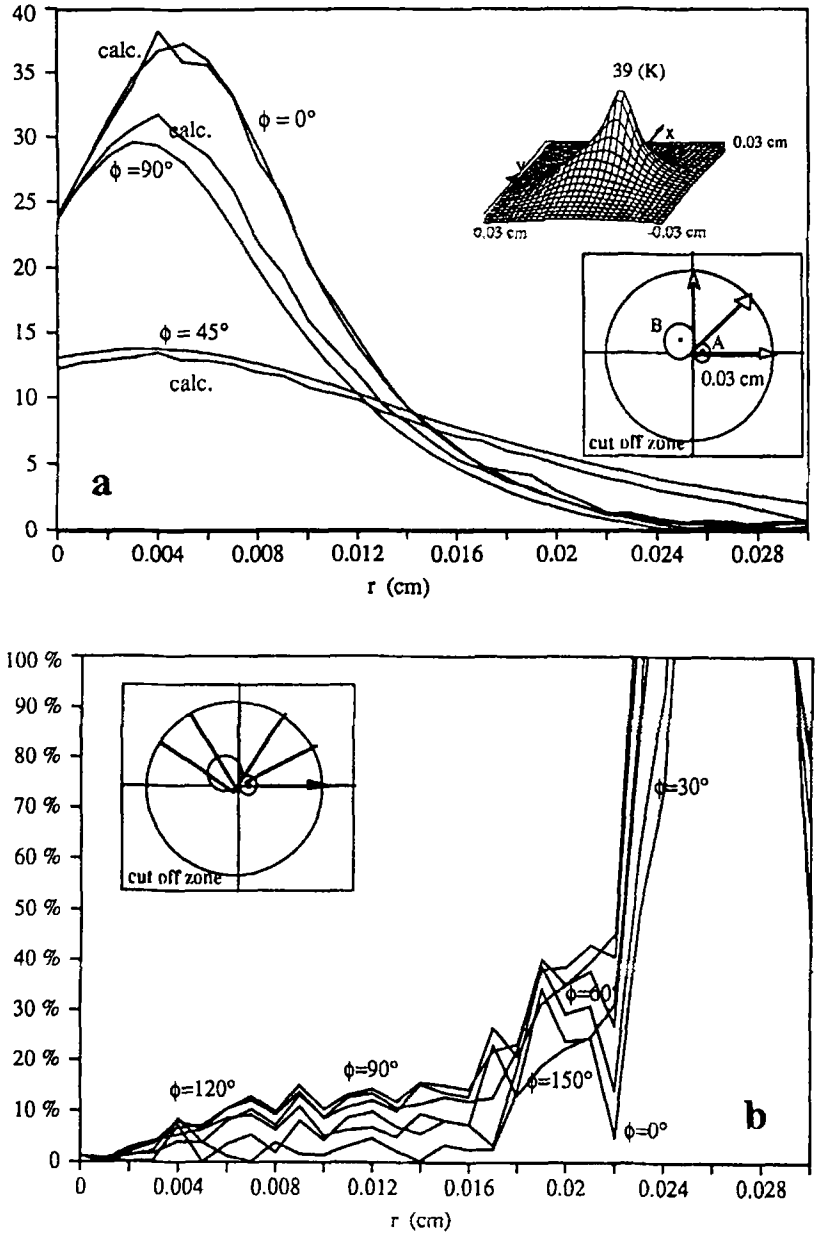

Fig. 5 Temperature profile for non symmetric case: (a) the amplitude of the temperature calculated from theory and from Eq. (11) for three different angles (0°, 45°, 90°). In the insert the temperature profile and the surface section. (b) the relative error between the temperature profiles calculated from theory and from Eq. (11) for a scanning system with $N=60$ and $M=24$, $\Delta_\phi=15°$, $\Delta=0.001$ cm

cally modulated in time at different frequencies (225–2500–10000–40000 Hz) in order to follow the dynamic of the heat transfer and hence to determine the thermal diffusivity. In Fig. 6 the amplitude of the deflection signal is plotted as a function of the distance y between the probe beam and the mirror (Fig. 7) with

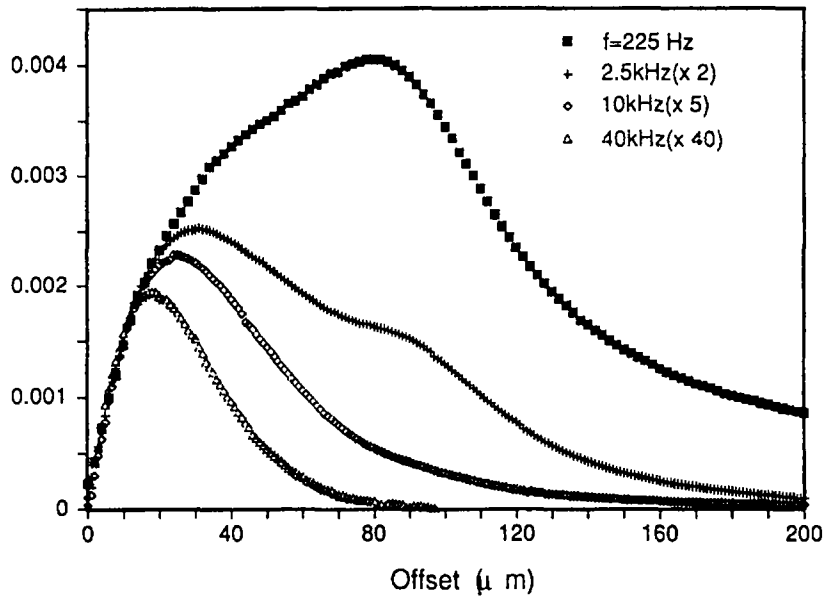

Fig. 6 The amplitude of the deflection signal *vs.* the distance from the mirror for a drive current 70 mA and for four different drive current modulation frequencies (■225 Hz; +2.5 kHz; ◊ 10 kHz; Δ 40 kHz) for AlGaAs laser diode

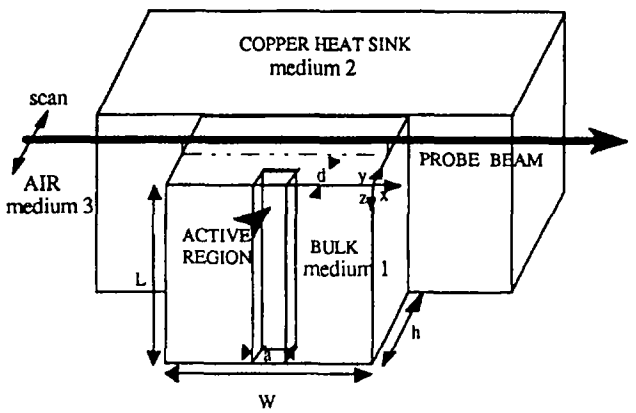

Fig. 7 Schematic representation of the geometry of the experiment on the laser diode; L – cavity length; a – stripe width; h=120 μm – bulk height; d – active region depth; w – bulk width; Probe beam-laser He – Ne, λ=632.8 nm, P=5 mW, spot-size 12 μm

a spatial step $\Delta=2$ μm. The deflection angles are finally obtained from the signal of the position sensor by multiplying for the response of the detection system $S=0.017$ rad/V.

In the experiment, the scan at the given step Δ, is performed along y axis from the air to the copper heat sink providing a set of N data. The phase is also shown in Fig. 8.

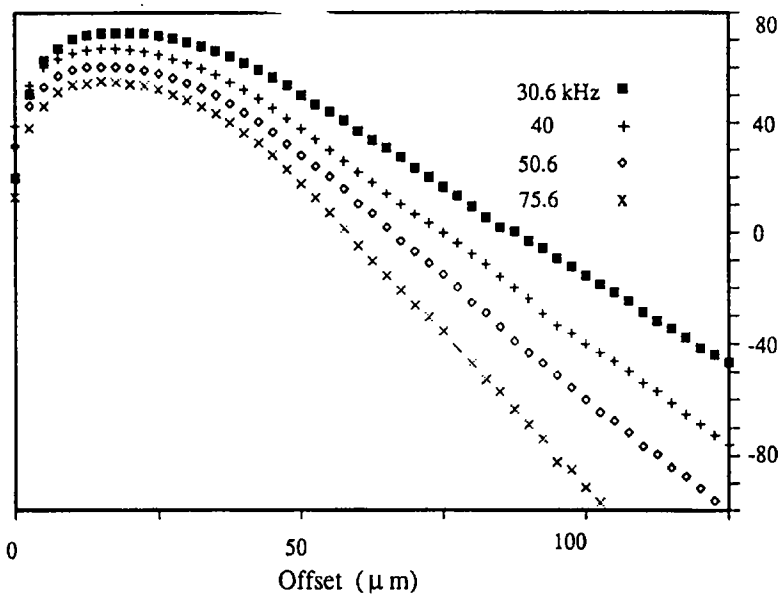

Fig. 8 The phase of the photodeflection angle as function of the scanning variable [y] for a drive current 70 mA and for different drive current modulation frequencies

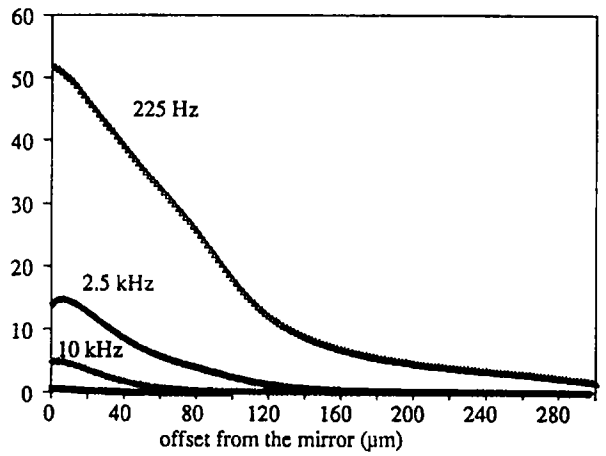

Fig. 9 Temperature profile of the semiconductor laser diode for four different frequencies (225 Hz, 2500 Hz, 10000 Hz, 40000 Hz)

By using Eq. (7) the temperature profiles are calculated and shown in Fig. 9 starting from the amplitude data of Fig. 6 and the phase data of Fig. 8 in the same spatial range with step $\Delta=2$ μm and for different frequencies of modulation. The maximum temperature rise of about 53±5 K is just on the mirror of the semiconductor laser cavity where the heat is mainly generated ($y\cong 0$) and increases for lower frequencies (Fig. 9).

Thermal conductivity measurements

The method to determine temperature profile has been successfully applied also to measure the thermal conductivity ratio between the copper heat sink and the semiconductor. In fact the temperature profile for $f=225$ Hz shows more clearly than the deflection signal, the existence of an interface between the copper heat sink near $y=120$ μm with a large but finite conductivity and the semiconductor monocrystal, through a sudden change in the slope. The different slopes found in the monocrystal and in the copper are directly connected with the thermal conductivity. In fact at the boundary semiconductor-copper, the thermal flux going into the copper has to be equal in the two media according with $k_1 dT_1/dy = k_2 dT_2/dy$. This consideration shows us that in the laser device DHS AlGaAs/GaAs the ratio $k_2/k_1 = dT_1/dT_2 \approx 10$.

This value, experimentally obtained, is in good agreement with the one found in the literature $k_{GaAs}=0.44\pm0.04$ and $k_{Cu}=4.01$ (W cm^{-1}K^{-1}) (relative error 10%).

The method applied in a very high frequency regime ($f > 30$ KHz) on the phase signal allows also to measure the thermal diffusivity of the device according to Eq. (4).

In fact, by plotting the phase of the deflection angle as a function of the offset y one obtains, according to the theory of phase method, a linear slope m (Fig. 9) which is related to the thermal diffusion length l and to the thermal diffusivity $D=0.28$ cm^2/s of GaAs. The accuracy of the phase method leads to an estimated error less than 5%.

Conclusions

The Photodeflection method is a powerful method for the determination of the thermal parameters of solids. Moreover how get thermal imaging from deflection angle has been shown. Experiments have been done for the determination of the temperature of a semiconductor laser diode.

References

1 A. C. Boccara, D. Fournier and J. Badoz, Appl. Phys. Lett., 36 (1980) 130.
2 Hall, A. W. Williams, 'A Photothermal Mirage Imaging System' – 8 ITMP^3 – Guadalupe 1994.

3 M. Bertolotti and R. Li Voti, G. Liakhou and C. Sibilia, Rev. Sci. Instrum., 64 (1993) 1576.
4 M. Bertolotti, R. Li Voti, G. L. Liakhou and C. Sibilia, Rev. Sci. Instrum., 66 (1995) 277.
5 C. Sibilia, M. Bertolotti, L. Fabbri, G. Liakhou and R. Li Voti – 'Thermal diffusivity Measurements in Multilayers through Photodeflection Method: Theory and Experiments' – Conference Proceedings Vol. 29 'Quantum Electronics and Plasma Physics' 6th Italian Conference – G. C. Righini (Ed.) SIF, Bologna 1991, p. 341, 349.
6 M. Bertolotti, R. Li Voti, F. Michelotti, G. Liakhou and C. Sibilia, J. Appl. Phys., 74 (1993) 7078.
7 M. Bertolotti, A. Ferrari, G. Liakhou, R. Li Voti, A. Marras, T. A. Ezquerra, F. J. Balta and C. Valleja, 'Thermal anisotropy of polymer carbon fiber composites as revealed by photodeflection methods', J. Appl. Phys., 78 (1995) 706.
8 M. Bertolotti, M. Firpo, A. Fontana, R. Li Voti and C. Sibilia, 'Analysis of defects in ceramics through photothermal deflection method' – SPIE Vol. 2248, 267.
9 X. Maldague and J. C. Krapez, 'Thermographic Nondestructive Evaluation: an Algorithm for Automatic Defect Extraction in Infrared Images' IEEE Transaction on systems, man and cybernetic, Vol. 20, n°3 May, June 1990.
10 L. J. Inglehart, A. Brøniatowski, D. Fournier, C. Boccara and F. Lepoutre, Appl. Phys. Lett., 56 (1990) 1749.
11 A. M. Mansanares, Z. Bozoki, T. Velinov, D. Fournier and C. Boccara, 'Photothermal reflectance microscopy: signal contrast in the case of thick and thin grain interfaces in solids' – 8 ITMP[3] Guadaloupe, 1994.
12 L. C. Aamodt and J. C. Murphy, J. Appl. Phys., 54 (1989).
13 M. Bertolotti, G. Liakhou, R. Li Voti, Ruo Peng Wang, C. Sibilia and V. P. Yakovlev, J. Appl. Phys., 74 (1993) 7054.
14 M. Bertolotti, G. Liakhou, R. Li Voti, C. Sibilia, A. Syrbu and R. P Wang, Appl. Phys. Lett., 65 (1994) 2266.
15 M. Bertolotti, G. Liakhou, R. Li Voti, Ruo Peng Wang, C. Sibilia and V. P. Yakovlev, Mirror temperature of semiconductor diode lasers studied with a photothermal deflection method – SPIE Vol. 2248, 335–344.